Transactions, SMiRT-23
Manchester, United Kingdom - August 10-14, 2015
Division X

ACCIDENT THERMAL LOADING EFFECTS ON SEISMIC BEHAVIOUR OF SAFETY-RELATED NUCLEAR STRUCTURES

Kadir C. Sener[1], Amit H. Varma[2] and Saahastaranshu R. Bhardwaj[3]

[1] Research Engineer, Lyles School of Civil Engineering, Purdue University, West Lafayette, IN, USA
[2] Professor, Lyles School of Civil Engineering, Purdue University, West Lafayette, IN, USA
[3] Ph.D. student, Lyles School of Civil Engineering, Purdue University, West Lafayette, IN 47906, USA

ABSTRACT

The Fukushima event of 2011 has highlighted the importance of designing safety-related nuclear facilities for accident thermal scenarios combined with design basis (safe shutdown) earthquake. While the probability of both events occurring simultaneously is low, severe environmental conditions may trigger accident thermal loading, and subsequent aftershocks, potentially as intense as the main shock, may occur during the accident thermal event. Current design codes and standards in the United States and abroad provide little-to-no guidance for including the effects of accident thermal loading on seismic behaviour (stiffness, strength, ductility or reserve margin) of structures. Prior research has focused on seismic behaviour or accident thermal loading but not both in combination. This is valid for both existing conventional reinforced concrete (RC) and modern steel-plate composite (SC) structures.

The authors have initiated a research project focussing on the effects of accident thermal scenarios on the in-plane shear behaviour (stiffness and strength) of SC and RC wall structures. This paper presents the initial findings from the project including: (i) typical temperature-time (*T-t*) curves for containment internal structures in pressurized water reactors, (ii) thermal gradient histories that develop through the concrete thickness, (iii) concrete cracking due to the severe gradient and internal restraint, (iv) in-plane shear behaviour of the wall after concrete cracking, and (v) effects of external restraints on the in-plane shear behaviour. The paper presents these findings related to both RC and SC walls, which are being used to develop the test matrix and parameters to be included in the experimental investigations that will be conducted in the next phase of the project.

INTRODUCTION

Structural walls are critical structural elements in Small Modular Reactors (SMRs) and Advanced Light Water Reactors (ALWRs) and their robust seismic performance is a key to seismic safety in design basis and beyond design basis earthquake shaking. Accordingly, this research focuses on the effects of accident thermal conditions on the seismic performance of innovative steel-plate composite (SC) walls and conventional reinforced concrete (RC) walls. The exterior steel faceplates of SC walls serve as reinforcement for the concrete section. The steel faceplates are anchored to the concrete using shear connectors (studs), and connected to each other using tie bars or rods. The steel faceplates (with no protection) are directly exposed to elevated temperatures resulting from accident thermal conditions. The differential temperatures between the steel faceplates and concrete infill, and the nonlinear thermal gradients lead to concrete cracking and potential overstressing of the steel faceplates (primary reinforcement) particularly during seismic events. For RC walls, the nonlinear temperature gradient through the thickness of the concrete section will lead to concrete cracking and significant stress in the steel rebar in the absence of earthquake shaking.

There are no design codes or standards for SC walls in the US although Supplement No.1 to AISC N690-12 [N690s1 (AISC 2014)], which is slated for release in 2015, will include Appendix N9 for their design. Neither this appendix nor its counterparts in Japan (JEAC 4681, 2009) and S. Korea (KEPIC-SNG, 2012) address the effects of accident thermal loading on seismic performance. Similarly, the much more established standard for safety-related RC structures, ACI 349-06 (2006), does not address the effects of accident thermal loading on the seismic performance of RC walls. Therefore, the overall goal of this research project is to develop knowledge-based design guidelines for safety-related nuclear facilities subjected to combined accident thermal conditions and seismic loading.

RESEARCH OBJECTIVES

The objective of this research article is to develop and benchmark numerical models for predicting the seismic performance of structural walls subjected to accident thermal loading and design basis and beyond design basis earthquake shaking. The models were developed and analyzed using sequentially coupled thermal-mechanical finite element analysis approaches with complete material nonlinearity including concrete cracking and steel plasticity.

Analytical parametric studies were conducted to comprehensively evaluate the effects of a wide range of parameters. The results from parametric studies were used to develop recommendations for calculating the pre and post cracked stiffness, and peak and post-peak strength response of structural walls exposed to accident thermal loading.

IDENTIFICATION OF ACCIDENT THERMAL LOADING HISTORY

The compartment temperature-time (*T-t*) histories result from postulated accident (pipe break) scenarios in the containment internal structures (CIS). Typical accident temperature-time histories for the CIS of nuclear power plants (NPPs) are identified using envelopes of *T-t* histories from publicly available Design Control Documents (DCD 2011, DCD 2012). Figure 1 presents the envelope temperature-time histories obtained for each major NPP compartment; e.g. reactor cavity, steam generator, refueling water storage pit, containment wall. As shown, the accident causes a sharp or sudden increase in temperature to a maximum value (ranging from 280°F-350°F), followed by cooling due to the dissipation of heat throughout the CIS. The elevated temperature is sustained over several days (approx. 15 days), but the curves were cut-off at 15 hours for clarity.

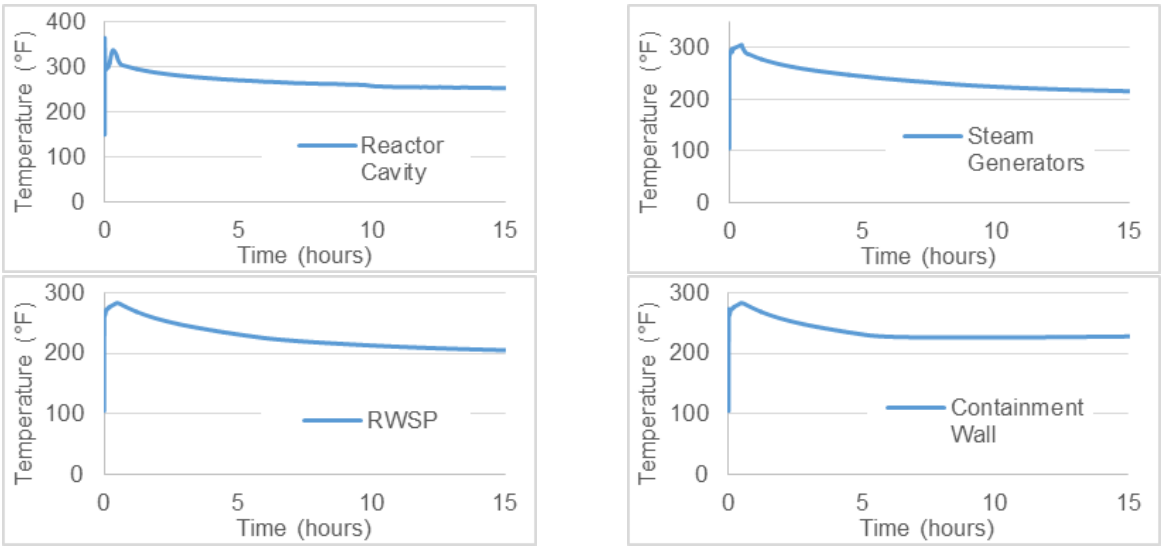

Figure 1. Temperature-time history envelopes for different NPP compartments

PRELIMINARY NUMERICAL ANALYSIS OF SC WALLS

Preliminary numerical models were built for development and benchmarking of numerical models to predict the nonlinear inelastic behavior of SC walls subjected to thermal loading and monotonic lateral loading. The preliminary models were benchmarked using the experimental data obtained in the literature from tests of in-plane shear behavior SC walls with and without thermal loading. The models were developed using the finite element method implemented in commercial and research programs such as ABAQUS (Dassault, 2013). The models were analyzed using sequentially coupled thermal-mechanical analysis approach as follows. Two similar finite element models were developed for conducting the nonlinear analysis: (i) heat transfer analysis, and (ii) inelastic stress analysis. The finite element meshes for both these analyses were identical so that the nodal temperature histories from the heat transfer analysis can be imported as thermal conditions to the stress analysis model. This thermal loading was applied to the stress analysis model before, after, or during the lateral loading analysis.

Numerical models with two different levels of complexity can be developed: (i) detailed 3D finite element models, and (ii) macro shell element models. The detailed 3D finite element models explicitly account for each of the components of the structural sections, and the various complexities of behavior. For the SC walls, the models can explicitly account for the steel faceplates, shear connectors, tie bars, concrete infill, and the interaction (normal and tangential) between the various elements. For the RC walls, the models can explicitly account for the steel reinforcing bars, shear stirrups, and concrete, and the interaction between the various elements. The macro shell finite element approach which is a simpler modeling approach is used in this preliminary study. The macro shell finite element model consists of multi-layered composite shell elements which are used to model the steel and concrete components using composite layers through the thickness. The shear connectors, tie bars and stirrups are not modeled explicitly. Full composite action is assumed between the steel and concrete layers. Material inelasticity for the steel and concrete layers including yielding, plasticity, and tension cracking features is incorporated in the models. Temperature-dependent thermal properties for steel and concrete are also accounted for in the macro shell element models similar to the detailed 3D models.

Benchmarking of Preliminary Models

The macro shell finite element models used in this parametric study were benchmarked using results from SC wall experiments conducted in Japan by Ozaki et al. (2004). The experiments that were conducted included shear panel tests at ambient and elevated temperatures. The test specimens included the following SC components: (i) steel faceplates, (ii) concrete infill, (iii) shear studs, and in some cases, (iv) tie rods. The benchmarking analysis discusses three unheated specimens (S200NN, S300NN, and S400NN), and the two corresponding heated specimens (S200TH and S400TH). All the test specimens had the same overall dimensions (47.2 in. x 47.2 in. x 7.87 in.), with slight differences in the steel faceplate thickness (t_p). The steel faceplate thicknesses were; 0.09 in, 0.126 in, 0.177 in for S200, S300 and S400 series specimens, respectively The tests were performed using a test setup that applied uniform in-plane shear forces to wall panels.

The heated specimens were subjected to thermal loading on both steel faceplates. The steel faceplates of the test specimens were heated up to 347°F (175°C) at a rate of 72°F/hour (40°C/hour) and then the temperature was maintained for 24 hours. After 24 hours, the specimen was left to cool naturally. After cooling, the specimens were subjected to in-plane shear loading using the same test setup to investigate the effects of heating on the in-plane shear behavior of SC walls.

The element type used in the finite element models was reduced (one) integration element as it makes the analysis computationally less expensive. Additionally, having only one integration point makes it simpler to physically understand the plastic strains or cracking strains associated with the finite element.

Steel behavior was modeled using multi-axial plasticity theory with: (i) Von Mises yield surface, (ii) associated flow rule, and (iii) isotropic hardening. The stress-strain curves for steel at different temperature magnitudes were generated according to the Euro code (CEN, 2001). The thermal properties of the steel, for instance, the thermal capacity and the thermal conductivity, were based on the Euro code (CEN, 2001) recommendations.

Concrete material model used for the concrete infill was smeared cracking model (CSC). CSC uses a linear Drucker-Prager compression yield surface with associated flow rule in compression. In tension, it uses a separate crack detection surface with oriented damaged elasticity to model smeared cracking. Temperature dependency of concrete mechanical properties were only accounted in the elastic modulus of concrete in accordance with NIST and Eurocode recommendations (Phan et al. 2010). The thermal properties of concrete, for instance, the thermal capacity and the thermal conductivity, were also based on the Euro code (CEN, 2001) recommendations. In order to completely define these models several parameters were required, such as; elastic modulus, Poisson's ratio and behavior in tension, compression and shear. The tension behavior was specified using a stress-crack opening displacement curve provided by CEB-FIB (1990) that is based on fracture energy and empirical models. The uniaxial compression stress-strain behavior of concrete is defined using the modified Popovic's empirical stress-strain model recommended by Collins et al. (1992).

Figure 2 presents the comparisons of analytically computed and experimentally measured shear force versus shear strain curves for the unheated (S200NN, S300NN, and S400NN) and heated (S200TH) specimens. The experimental results for specimen S400TH was not reported due to machine malfunction during the test. The figures illustrate that the simplified (macro shell finite element) analytical models predict the behavior of the specimens reasonably up to yielding, and conservatively after yielding. The figure also includes the analytically computed shear force versus strain curve of Specimen S200NN and Specimens S200TH for comparison. The comparisons between the analytically computed curves indicate that the heated specimen had lower initial stiffness due to the cracking of concrete in the heating phase prior to the mechanical loading. However, the ultimate strength difference between the heated and ambient cases were negligible. The benchmarking analysis results for shear panel tests indicate that the macro shell finite element model can be used to predict the behavior of SC shear walls with acceptable accuracy and conservatism for preliminary studies.

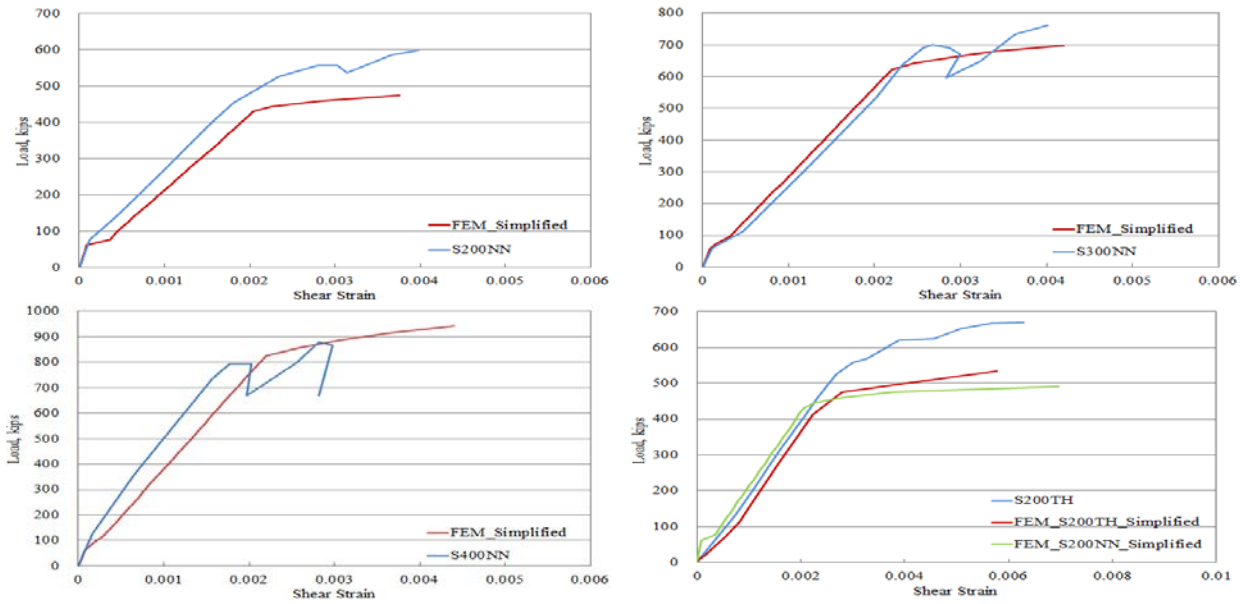

Figure 2. Shear force-shear strain responses from experiments and analysis results

ANALYTICAL PARAMETRIC STUDIES

The benchmarked finite element models were used to conduct analytical parametric studies of SC wall panels. The study included reinforcement ratio as the geometric parameter, which is calculated as the ratio of total steel area to the cross sectional area ($\rho=2t_p/T$, where t_p is the faceplate thickness and T is the section depth), Four different reinforcement ratio values were used (ρ=1.5%, 2%, 3%, and 4%). The reinforcement ratios were selected based on the common reinforcement ratio levels used in safety-related nuclear facilities. Additionally, three temperature amplitudes were used in this parametric study. The temperature amplitudes were T=150°F (65.6°C), T=300°F (148.9°C) and T=450°F (232.2°C), and were applied to the steel surfaces on both sides of SC walls where the room (ambient) temperature was taken to be T_0=50°F (10°C). The SC wall panels analyzed in this parametric study were 8 ft. x 8 ft. in height and width, and 4 ft. thick. The wall dimensions used in the analytical model were taken comparable to the sizes used in actual containment structures (DCD 2011, DCD 2012). The steel faceplates yield strength was taken as f_y = 58 ksi (396 MPa, ε_y=2000$\mu\varepsilon$), and the concrete compressive strength was f'_c = 6 ksi (41.4 MPa).

The parametric study models a combined in-plane shear + thermal loading scenario. The loading protocol in the analytical models included three steps with; (i) a mechanical loading that is sufficient to initiate shear cracking in concrete, (ii) the nodal temperatures from the heat analysis results were applied to the stress analysis model, (iii) finally the mechanical load was gradually increased to the final force capacity as the temperatures of each node were maintained. This loading history was found to result in the lower bound strength mainly because of initiating concrete cracking in the first loading phase and then extending the existing cracks or forming additional cracking due to heating. Experiments conducted by the authors (Varma et al., 2013) on SC wall beams have confirmed that the loading protocol provided lower bound shear strength. The sequence and duration of mechanical and thermal loading histories used in the models is illustrated in Figure 3.

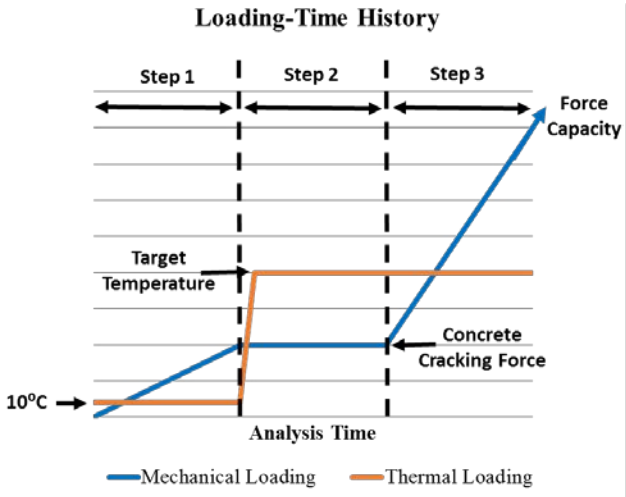

Figure 3. Mechanical and thermal loading history used in models

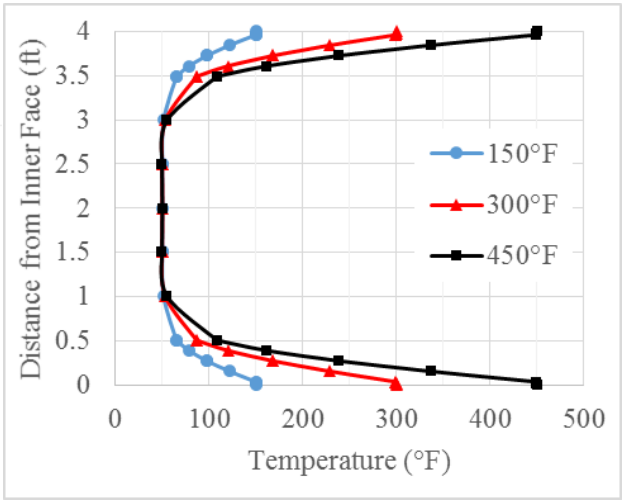

Figure 4. Temperature variation thru-thickness of SC walls

The steel faceplate surfaces of the finite element models (exterior layers) were heated to the target temperature in 20 minutes. The temperature was maintained constant for 160 minutes (to achieve 3 hours of heating). The temperature variation through the depth of 4ft thick SC section is shown in Figure 4, for the target temperatures (150°F, 300°F and 450°F) at the end of 3 hours. As seen in Figure 4, a nonlinear temperature gradient through the cross section is observed with a steep variation from target temperature on the surfaces to ambient temperature in the mid-height of the section.

Representative Analysis Results

The analysis results of SC panel with 2% and 4% reinforcement ratios (ρ) at ambient and elevated temperature cases are discussed in this section. The observed behavior was similar for other reinforcement ratios. Pure in-plane shear loading was applied to the four edges of the SC wall panels generating principal tension and compression stresses directed perpendicularly. In order to provide more insights into the observed shear behavior, the panel shear strain, principal concrete compression stress (S_{min}) and equivalent plastic strain in steel (*PEEQ*) variations are observed with increasing panel shear force. Shear strain variation through the thickness was identical in all layers due to absence of any out-of-plane curvature through the panel thickness.

Figure 5(a) shows the panel shear strain, steel plastic strain (*PEEQ*) and concrete compressive stress (S_{min}) change with the applied in-plane shear force for the 2% reinforcement ratio panel at ambient condition. The figure indicates that the concrete compressive stress increases with the applied force. Slope of the shear force vs. S_{min} curve changes at approximately 1000 kips, after the occurrence of tensile cracking in the principal tension stress direction. After the cracking, the slope of the compressive stress curve is nearly constant until the initiation of yielding in the faceplates, where the steel plastic strains indicate their first increase. The concrete cracking and steel faceplate yielding load levels are also observed in the shear force vs. panel shear strain curve as it reflects as slope changes on the curve. The shear force capacity of the panel is reached shortly after the yielding of the steel faceplates.

Figures 5 (b), (c), and (d) show the panel shear strain, steel plastic strain and concrete compressive stress variation following the loading sequence given in Figure 3 for target temperatures 150ºF, 300ºF and 450ºF, respectively. The thermal loading is applied while the initial mechanical load remains constant, which initial shear cracking had already occurred prior to the heating. The panel mechanical strain ($\varepsilon_{mech} = \varepsilon_{tot} - \varepsilon_{th}$) in both principal directions become tensile due to the thermal expansion (thermal strains) of the panel. This can be interpreted as compression zones turning into tension zones (possibly cracking in tension) due the panel not having any restraint for thermal expansion. Another consequence of the thermal expansion is that the concrete infill losing its contribution to the panel shear force. Therefore, a jump in the shear strain of the panel is observed during the heating phase although the applied shear force is constant. The strain jump is due to force redistribution in the SC wall panel. Steel faceplates resist the shear force that was carried by the concrete infill, which causes additional shear strain in the panel.

As the shear loading is resumed in loading step 3 (see Figure 3), the concrete compressive stress do not increase until the tensile strains turn back into compressive strains, in other words until the crack closure in the principal compression direction. The panel shear stiffness increases slightly after the concrete infill starts contributing to shear resistance (resisting compressive stresses). Steel faceplate yielding occurs at a lower shear force level compared to the ambient case, due to the concrete infill not carrying shear force as effectively after the thermal loading and additional forces are resisted by the faceplates.

Figures 5(c) and (d) show the response curves for the 300 ºF and 450 ºF thermal loading case. In these cases yielding of the steel faceplate occurs at a lower load level than the 150ºF case due to concrete not carrying compression until the faceplate yielding. Unrestrained thermal strains cause cracking in the principal compression direction and concrete contribution begins only after the crack closure. The figures also show the calculated shear stiffness contribution of the steel faceplates only ($K_s = G_s A_s$, where G_s.is the steel shear stiffness and A_s is the faceplate cross-sectional area) The analytically obtained panel shear stiffness and the calculated shear stiffness of the steel faceplates (K_s) are in good agreement as shown in the figures. The comparison of stiffnesses indicates that while concrete cannot resist compression, the only contribution to resist the shear force is provided by the steel faceplates. Increase in the shear force after the yielding causes concrete to start resisting compressive stresses. This delayed contribution of the concrete infill is observed as an increase in the shear stiffness of the SC wall panel.

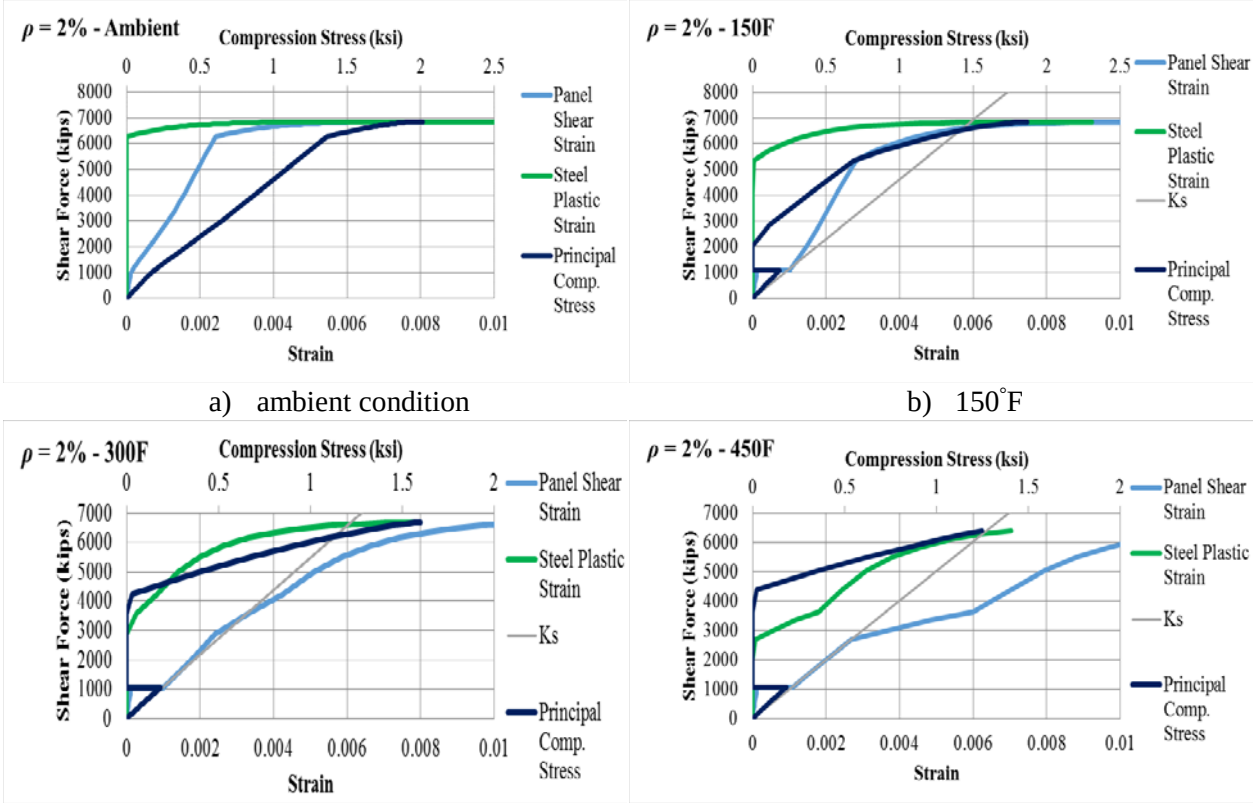

Figure 5. Panel shear strain, steel plastic strain, concrete compression stress variations of SC panel

Parametric Study Results

Figure 6 shows some sample results from macro shell finite element analyses of SC wall panels subjected to accident thermal loading followed by mechanical loading. The figure includes the in-plane shear force-shear strain responses for SC walls with 4% reinforcement ratio. It includes the response for ambient conditions, 150˚F, 300˚F and 450˚F maximum temperature. The heating for all three cases was applied for three hours. As shown, accident thermal conditions have significant influence on the in-plane shear stiffness, strength, and deformation capacity of SC walls. The tri-linear mechanics-based model proposed by Varma et al. (2011) for in-plane behavior of SC walls is also compared with the analysis results. The tri-linear model is developed using equations for the cracking and ultimate strength (S_{ct}, $S_{xy}^{\gamma} = V_{max}$) and cracked and uncracked stiffness (K_{xy}^{uncr}, K_{xy}^{cr}) of SC walls. The equations used to develop the tri-linear curve are given from Equations (1) to (4). The comparisons indicate close agreement between the tri-linear model and ambient analysis results. The figure shows the (i) strain jump for the heated models during the thermal loading, and (ii) post-heating response of the panel shear force-shear strain relationship.

$$K_{xy}^{uncr} = G_s A_s + G_c A_c \qquad (1)$$

$$S_{ct} = \frac{2\sqrt{f'_c}}{1000}\left(\frac{E_c A_c + E_s A_s}{E_c}\right)(psi) \qquad (2)$$

$$K_{xy}^{cr} = \frac{1}{\frac{4}{0.7E_c A_c} + \frac{2(1-\nu_s)}{E_s A_s}} + G_s A_s \qquad (3)$$

$$S_{xy}^{\gamma} = \frac{K_s + K_{sc}}{\sqrt{3K_s^2 + K_{sc}^2}} \times A_s F_y \qquad (4)$$

The SC wall panel models were free to expand without any edge restrain when exposed to heating, which is not realistic for walls used in actual structures. SC walls are typically restrained to deformations along the edges. The edge restrains would occur due to connections with adjacent walls on the side edges, and connections with the foundation or floor slabs on the top and bottom edges. These connections are expected to introduce some level of translational restraints on the edges of the panels, which may result in significant reduction in the thermal expansion of the walls. Therefore, restraint levels were introduced to the wall panel models to study the edge restraint influence on the in-plane + thermal behavior of SC wall panels. In this study three restraint levels, viz. 100% (full), 50% (half) and 25% (quarter), were applied to each SC wall panel at different temperature conditions. Figure 7 shows the effect of restraint on the shear force vs. shear strain response for SC walls with 4% reinforcement ratio and heated to 150˚F. The figure shows that increased restraint diminishes the strain jump that occurs in the heating phase and vanishes for the full restraint (100%) case. The post-cracked shear stiffness and strength of the panel also increases with larger restraint levels.

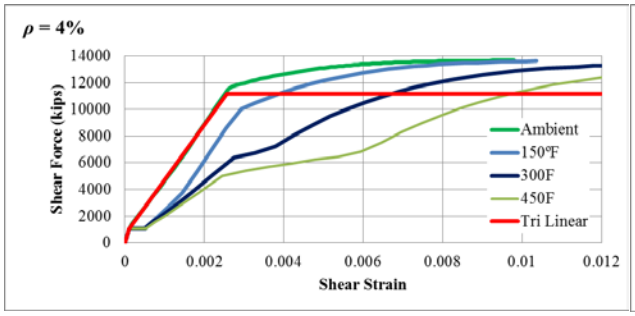

Figure 6. Shear force vs. shear strain comparisons of SC panels at different thermal loading

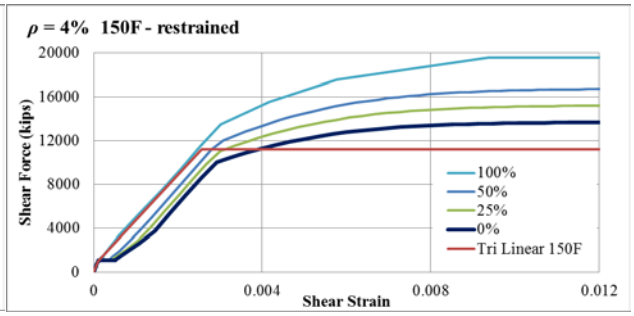

Figure 7. Shear force vs. shear strain comparisons of SC panels with different restraint conditions

The desired level of restraint was achieved by applying shell edge load normal to the edge on all four edges of the SC wall panels. The required force for each restraint level was calculated based on the force needed for full restraint at each target temperature. The full restraint was obtained by applying the reaction forces of a heated panel that is translationally constrained at all four sides. In a fully restrained wall, the panel does not experience any thermal expansion (ε_{tot}=0). Restraint levels 50% and 25% were obtained by applying half and quarter of the force magnitude of the full restraint case, respectively.

Table 1 provides numerically compared results from the parametric study. The results are normalized with the panel shear strength calculated based on the tri-linear model (Eq. 4) accounting for temperature dependent material properties. The analytical panel strength is defined as the force that corresponds to the panel shear strain of 0.6%. This level of shear strain was found to be a reasonable representation of the panel strength, because it corresponds (i) to steel plastic strain (*PEEQ*) of approximately 0.2% and (ii) to a principal concrete compression stress (S_{min}) of less than 50% of the specified compressive strength of concrete (f'_c).

Table 1: Strength comparisons of SC panels with different reinforcement ratios

	$V_{max}^{\rho=1.5\%}$ / Eq. 4				$V_{max}^{\rho=2\%}$ / Eq. 4				$V_{max}^{\rho=3\%}$ / Eq. 4				$V_{max}^{\rho=4\%}$ / Eq. 4			
Rest.	Amb.	150ºF	300ºF	450ºF	Amb.	150ºF	300ºF	450ºF	Amb.	150ºF	300ºF	450ºF	Amb.	150ºF	300ºF	450ºF
0%	1.09	1.01	0.95	0.54	1.12	1.09	0.91	0.61	1.16	1.12	0.94	0.66	1.20	1.14	0.96	0.63
25%		1.23	1.24	0.72		1.24	1.19	0.96		1.27	1.18	0.93		1.26	1.17	0.86
50%		1.39	1.51	1.40		1.40	1.46	1.32		1.40	1.36	1.27		1.37	1.42	1.15
100%		1.71	2.11	2.34		1.65	1.79	1.81		1.61	2.01	2.04		1.57	1.60	1.82

OBSERVATIONS & CONCLUSIONS

The authors have initiated a research project focussing on the effects of accident thermal scenarios on the in-plane shear behaviour (stiffness and strength) of SC and RC wall structures. This paper presents the initial findings from the project including: (i) typical temperature-time (*T-t*) curves for containment internal structures in pressurized water reactors, (ii) thermal gradient histories that develop through the concrete thickness, (iii) concrete cracking due to the severe gradient and internal restraint, (iv) in-plane shear behaviour of the wall after concrete cracking, and (v) effects of external restraints on the in-plane shear behaviour. The paper presented these findings prior to future experimental investigations that will be conducted in the next phase of the project.

The effect of accident thermal loading on the seismic performance of SC or RC walls has not been investigated experimentally or numerically. Prior research has focused on either seismic behavior or accident thermal loading but not both in combination. The combination of accident thermal loading and safe shutdown earthquake (SSE) will present a significant design challenge for containment structures of safety-related nuclear facilities because postulated accident scenarios will cause elevated temperatures for long durations in their constrained spaces. For approval, the regulator will require extensive technical information and clear evidence of safety for the accident thermal + SSE loading combination, which may compromise the licensing schedule.

The project outcomes will include fundamental knowledge in terms of experimental results, benchmarked numerical models, and analytical results regarding the influence of accident thermal conditions and various parameters on the seismic behavior (stiffness, strength, and ductility) of SC and RC walls. This knowledge will enable future regulation of SMRs and ALWRS through validated recommendations for analysis and design for combined accident thermal and earthquake loadings, suitable for consideration by committees of ACI 349 and AISC N690. The knowledge could also be applied to existing nuclear power plants and structures in the DOE complex.

The analysis results of this study show that the reinforcement ratio and temperature amplitude have remarkable influence on the behavior of SC walls. Thermal loading affects the in-plane shear stiffness and strength of SC composite walls. Both shear stiffness and shear strength are reduced at elevated temperature and becomes more significant at high temperature amplitudes (300ºF and 450ºF). The tri-linear approach by Varma et al. (2011) can be used to predict the behavior of SC walls subjected to combined thermal + in-plane shear loading due to being conservative for most of the realistically restrained SC wall panel model cases.

The in-plane stiffness and shear strength of SC walls increase with the increase in reinforcement ratio. The pre-cracking branch is almost identical for all reinforcement levels. A slight deviation occurs in the cracked stiffness and ultimate strength; however, less than 20% difference was seen in most of the cases and the tri-linear equation was always on the conservative side. Shear force vs. shear strain curves obtained from the FE models for the higher temperature levels of 300ºF and 450ºF show different in-plane shear behavior mainly due to delayed shear contribution of the concrete infill. This delay occurs due to the thermal loading phase, where new cracks form in concrete due to the thermal expansion of the unrestrained SC wall panel. Until these cracks close with the increased shear loading, the panel shear stiffness is resisted only by the steel faceplates. The cracked stiffness of the 300ºF and 450ºF cases were about 60% of the cracked stiffness from the ambient condition, the concrete cracks eventually close and therefore the ultimate strength compares well with an average 10% difference vs. ambient.

Unrestrained SC wall panel case is not likely to occur when used in structures due to connections with other structural members such as foundations, other wall members, or slabs. In order to model a more realistic scenario, edge restraints were applied to panels by means of axial shell edge loads to prevent or

diminish the thermal expansion of SC walls. Three restraint levels were chosen for this study, including 25%, 50% and full restraint (100%). The full restraint condition is not likely to be observed in SC walls used in structures, since it indicates the case for no thermal displacement in the thermal loading phase. The other two restraint cases were essentially obtained by scaling the shell edge load calculated to provide full restraint.

The shear stiffness comparisons indicate that the 25% and 50% restraint cases result in similar stiffness as the unrestrained case. The strength increase for the 25% restraint case is about 20% from the unrestrained case, which is about 120% of the strength tri-linear equation (S_{xy}'). The 50% restraint case provides strength about 1.4 times the tri-linear approach. Lastly, the full restraint case, which is the other extreme and not likely to occur in structures, has shown to significantly overestimate both the stiffness and strength by a factor of two.

ACKNOWLEDGMENTS

The research is funded through the FY 2014 Nuclear Energy Enabling Technologies Research & Development and Infrastructure Awards by the U.S. Deparment of Energy, grant no: DOE-ID-14-032.

REFERENCES

ACI 349-06 (2006). *Code Requirements for Nuclear Safety-Related Concrete Structures and Commentary.* American Concrete Institute, Farmington Hills, MI.

American Institute of Steel Construction (2014). *Specification for Safety-Related Steel Structures for Nuclear Facilities Supplement No. 1*. AISC N690s1. PUBLIC REVIEW DRAFT DATED 5-1-14. American Institute of Steel Construction, Chicago, IL.

CEB-FIP Model Code (1990). "First complete draft", fib bulletins 55 and 56, International Federation for Structural Concrete (fib), ISBN 978-2-88394-095-6 and ISBN 978-2- 88394-096-3

CEN (European Committee for Standardisation), (2001), *Eurocode 1: Actions on Structures*, Part 1.2: General Actions – Actions on Structures Exposed to Fire.

Collins M, Mitchell D, MacGregor J. (1992). "Structural design considerations for high strength concrete", *Network of Centers of Excellence on High Performance Concrete*, Toronto, Canada

Dassault, (2013). *ABAQUS Analysis User's Manual*, Version 6.13. Providence, RI: Dassault Systèmes Simulia Corp

DCD (2011). "Design control document for the AP1000.": *U.S. Nuclear Regulatory Commission*, Washington, DC, USA. [http://www.nrc.gov/reactors/new-reactors/design-cert/ap1000.html].

DCD (2012). "Design control document for the US-APWR." *U.S. Nuclear Regulatory Commission*, Washington, DC, USA. [http://www.nrc.gov/reactors/new-reactors/design-cert/apwr.html].

JEAC 4618 (2009). *Technical Code for Seismic Design of Steel Plate Reinforced Concrete Structures: Buildings and Structures.* Japanese Electric Association Nuclear Standards Committee, Tokyo, Japan

KEPIC-SNG (2012). *Specification for Safety-Related Steel Plate Concrete Structures for Nuclear Facilities*. Board of KEPIC Policy, Structural Committee, Korea Electric Association.

Ozaki, M., Akita, S., Oosuga, H., Nakayama, T., Adachi, N. (2004). "Study on Steel Plate Reinforced Concrete Panels Subjected to Cyclic In-Plane Shear." *Nuclear Eng. and Design*, Vol. 228, pp. 225-244

Phan, L.T., McAllister, T.P., and Gross, J.L. (2010). "Best practice guidelines for structural fire resistance design of concrete and steel buildings." *NIST TN 1681*, Gaithersburg, MD.

Varma, A.H., Zhang, K., Chi, H., Booth, P.N., and Baker, T. (2011). "In-Plane Shear Behavior of SC Composite Walls: Theory vs. Experiment." *Trans of SMiRT 21*, IASMiRT, NCSU, Raleigh, NC.

Varma, A.H., Sener, K., and Winkler, D. (2013). "Behavior and Design of SC Composite Walls for Accident Thermal Loading." *Trans. of SMiRT 22*, IASMIRT, NCSU, Raleigh, NC.